ELSEVIER

Chemical Geology 170 (2000) 113–131

CHEMICAL GEOLOGY
INCLUDING
ISOTOPE GEOSCIENCE

www.elsevier.com/locate/chemgeo

Crystal chemistry of suspended matter in a tropical hydrosystem, Nyong basin (Cameroon, Africa)

Gwenaelle Olivié-Lauquet [a,*], Thierry Allard [a], Jacques Bertaux [b], Jean-Pierre Muller [a,b]

[a] *Laboratoire de Minéralogie-Cristallographie, Universités Paris 6 et 7, UMR CNRS 7590 et IPGP, 4, Place Jussieu, 75252 Paris Cedex 05, France*

[b] *O.R.S.T.O.M., Centre d'Ile de France, 32, Avenue Henri Varagnat, 93143 Bondy Cedex, France*

Received 27 June 1998; accepted 19 April 1999

Abstract

Suspended matter (SM) from the Nyong basin (Cameroon, Africa), a tropical watershed, was collected by tangential flow ultrafiltration to separate particulate (> 0.45 μm) and colloidal (< 0.45 μm; > 20 kDa) fractions. In this basin, two distinctive systems in a selected small catchment (Nsimi–Zoétélé) of the Nyong river basin have been considered: (i) colourless water (groundwater and spring) with a low suspended load (< 3 mg/l) and a low total organic carbon content (TOC < 1 mg/l) and (ii) coloured water (Mengong brook and Nyong river), which is organic rich (TOC > 10 mg/l) and contains higher amounts of SM (10–20 mg/l) than the colourless water. Freeze-dried samples of SM have been analysed by X-ray diffraction (XRD), transmission electron microscopy (TEM), Fourier-transform infrared spectroscopy (FTIR), electron paramagnetic resonance spectroscopy (EPR), and visible diffuse reflectance spectroscopy (DRS).

Colourless water mainly contains mineral phases, such as poorly ordered kaolinite, plus quartz and goethite in the particulate fraction, and euhedral kaolinite plus amorphous iron oxyhydroxides in the colloidal fraction. In contrast, the SM in coloured water is mainly organic in nature. The mineral phases in the particulate fraction are similar to those from clear water, but with additional phytoliths and diatom frustules composed of biogenic opal. In the colloidal fraction, complexation of Fe^{3+} and Mn^{2+} with organic matter is evidenced by EPR, together with significant occurrence of Fe oxyhydroxides associated with organic matter.

The sites of Al, Si, Fe, Mn in colloidal fractions derived from spectroscopic analyses are discussed with reference to chemical analyses performed by inductively coupled plasma mass spectrometry. Most of the observed solid phases or species correspond to those expected from published thermodynamic calculations for the same hydrosystem, except the colloidal iron oxyhydroxides in the coloured water. The presence of such iron phases is emphasised since they are expected to have large sorption capacities for numerous trace elements.

* Corresponding author. Laboratoire de Géochimie, Geosciences Rennes, Campus Beaulieu, 35042 Rennes Cedex, France. Fax: +33-2-9928-1499.

E-mail address: lauquet@univ-rennes1.fr (G. Olivié-Lauquet).

0009-2541/00/$ - see front matter
PII: S0009-2541(99)00244-2

The crystal chemistry of SM is used to discuss the origin of the mineral particles transported from the soil to the main rivers in terms of mechanical and chemical erosion processes.

Keywords: Suspended matter; Colloids; FTIR spectroscopy; Electron paramagnetic resonance spectroscopy; X-ray diffraction; Diffuse reflectance spectroscopy; Tropical watershed

1. Introduction

Rivers transport the products of erosion either in a dissolved form (chemical erosion) or in a solid form (physical erosion) (e.g., Eisma, 1993; Gaillardet et al., 1995). Although most studies have focused on the chemistry of dissolved loads in natural water, it has become increasingly obvious that inorganic and organic suspended matter (SM), in both the particulate and colloidal fractions, plays an important role in the transport and fate of trace elements, organic compounds and nutrients (e.g., Salomons and Forstner, 1984; Buffle and Van Leuwen, 1992). A few studies have been devoted to the nature and role of the smaller, colloidal fractions, which, due to their small size, large specific surface areas and high surface free energies, may play a major role in the scavenging of dissolved species (e.g., Sholkovitz, 1992; Dai and Martin, 1995; Viers et al., 1997). Two major difficulties have been encountered when studying the particulate and colloidal matter transported in rivers. The first difficulty arises from their low concentrations, and the second from their composition. Difficulties arising from low concentrations (several mg/l) have been partly overcome because new techniques are now available to collect and separate natural SM in aquatic systems (Buffle and Van Leuwen, 1992). Descriptions of SM available in the literature suggest that coarse as well as submicron particles in the oxygenated water of rivers are mainly composed of organic matter and various mineral phases, which are commonly poorly ordered (e.g., silica, iron oxyhydroxides and clays) (Gibbs, 1973; Buffle and Van Leuwen, 1992). Investigation of the nature of mineral phases and sites of trace elements in suspended sediments requires a chemical probe with both a low detection limit for specific trace elements and high sensitivity to local structures. Three methods, Fourier-transform infrared spectroscopy (FTIR), electron paramagnetic resonance (EPR), and UV–VIS spectroscopy in diffuse reflectance mode (DRS) applied to solids, are suitable for this type of analysis. These techniques are complementary to classical mineralogical techniques, such as X-ray diffraction (XRD) and transmission electron microscopy (TEM). These nondestructive spectroscopic techniques have provided evidence for the actual sites of trace components in clay minerals or identification of amorphous phases (e.g., Hawthorne, 1988). FTIR spectroscopy permits analysis of naturally occurring organic groups, of associated clay minerals and silica phases (either crystalline or amorphous) and of organo-metal complexes (Farmer and Palmieri, 1975; Senesi, 1992 and the reference therein). In addition to FTIR, EPR spectroscopy has been widely exploited for the determination of complexes between transition metals (e.g., Fe, Mn, Cu, etc.) and natural organic compounds (Cheshire and Senesi, 1998 and references therein). Moreover, it has been used for the crystal-chemical investigation of various clay minerals, including kaolinite resulting from lateritic weathering (Goodman and Hall, 1994; Muller et al., 1995). EPR analyses of SM or sediments from terrestrial or marine water improved understanding of the mechanisms that govern partitioning of specific elements, such as Fe^{3+} and Mn^{2+} between water and solids (Burgess et al., 1975; Bourghriet et al., 1992; Olivié-Lauquet et al., 1999). Finally, DRS may be used for identification of crystalline and amorphous iron and titanium oxides at very low concentrations in materials from the Earth's surface (Malengreau et al., 1994, 1995).

The present study is specifically designed to provide detailed information on the nature of SM from a tropical hydrosystem, specifically a small watershed (Nsimi–Zoétélé) located in the Nyong river basin (Cameroon, Africa). In the studied area, streams carrying dominantly organic SM drain a deep lateritic mantle beneath the tropical forest. A geochemical study of the water was performed by Viers et al. (1997), who first characterised the mechanisms that

control weathering processes for several major and trace elements. The present study, using XRD, TEM, FTIR, EPR, DRS analyses, provides complementary results to the previous study on the nature and origin of the SM. Particular emphasis has been placed on: (i) the sources and the mechanisms of transfer of Si, Fe and Al, which are major elements of lateritic weathering crusts, and Mn, which is an important redox tracer (De Vitre and Davison, 1993); and (ii) the Fe oxides and the organic matter, which play a major role in geochemistry of trace metals (Jenne, 1968; Eyrolle et al., 1996). The results of this study are important not only to supplement the mineralogical database related to tropical rivers, but also to provide direct evidence for the role of colloids in the geochemistry of some trace metals.

2. Study area

2.1. The Nyong hydrographical system and the Nsimi–Zoétélé watershed

The Nyong river basin (28,000 km^2), located between 2°48′N and 4°32′N latitude (Fig. 1A) belongs to the ''South Cameroonian Plateau'', i.e., an erosion surface characterised by small, rounded hills, which are covered by a tropical rain forest and separated by flat swamps. The Nsimi–Zoétélé catchment (Viers et al., 1997), about 60 ha in size, belongs to the Nyong river hydrographical network (Fig. 1B). It consists of two convex hills covered by semideciduous rain forest, which has been partially cleared for farmlands. The hills surround a swampy zone representing about 20% of the basin aera (Fig. 1C) and covered by raphia palm trees. At the head of this catchment, several springs give rise to the Mengong, a small brook about 1 km long flowing through the swampy zone. The humid tropical climate of the region is marked by two dry and two wet seasons of unequal duration.

2.2. The parent rock and the soil system

The regolith of the Nyong basin consists in part of polycyclic lateritic formations that developed from alteration of granites of the Ntem Plutonic Complex (2800 Ma, Bessoles, 1980). Petrological and mineralogical characteristics of these formations have been studied in detail at eleven pits, 2 to 15 m deep, in a soil toposequence located within the Nsimi–Zoétélé catchment (L6; Fig. 1C). These soils are representative of the lateritic mantle, which makes up the ''half-an-orange'' hills that form in tropical, humid climates under forest cover in Central Africa, South America and Asia.

Along a zone two-thirds of the way up the hills, weathering profiles are comprised of three superimposed horizons, which from the base to the top are: a lower saprolite zone, an intermediate ferruginous nodular zone and an upper yellow clayey zone. Downslope, the nodular horizon is progressively replaced by a thick indurated ferruginous horizon (hardcap). Material from these zones has a monotonous mineralogy and is predominantly comprised of quartz, kaolinite, and crystalline Fe-and Al-oxyhydroxides (goethite, hematite and, to a lesser extent, gibbsite). Further details on the mineralogy of similar types of weathered horizons have been described previously (Muller and Calas 1993a and references therein) for the Goyoum toposequence (East Cameroon).

The swampy zone exhibits hydromorphic soil profiles comprised of, from the base to top: alternating lenses of clay-dominated and sandy materials, an intermediate zone composed of bleached kaolinitic clays and quartz, and a brown silt–clay horizon rich in organic matter. The thickness of these soils is variable and ranges from 1 and 15 m.

2.3. Water characteristics and sampling sites

The Nyong basin is a ''transport-limited system'' (Stallard, 1988) since it is characterised by shallow slopes and a deep lateritic weathering mantle. A striking characteristic of natural water from this basin is that the groundwaters, which drains the lateritic crust, is colourless, whereas the brook and river water (i.e., from the Mengong to the Nyong; see Fig. 1B) are strongly coloured by organic matter (Viers et al., 1997).

Colourless groundwaters was collected in two localities: (i) in pit 8 of the L6 toposequence, at 2 m depth; and (ii) in one of the springs (Fig. 1C). Soil materials drained by the groundwater are expected to be an important source of SM and have also been

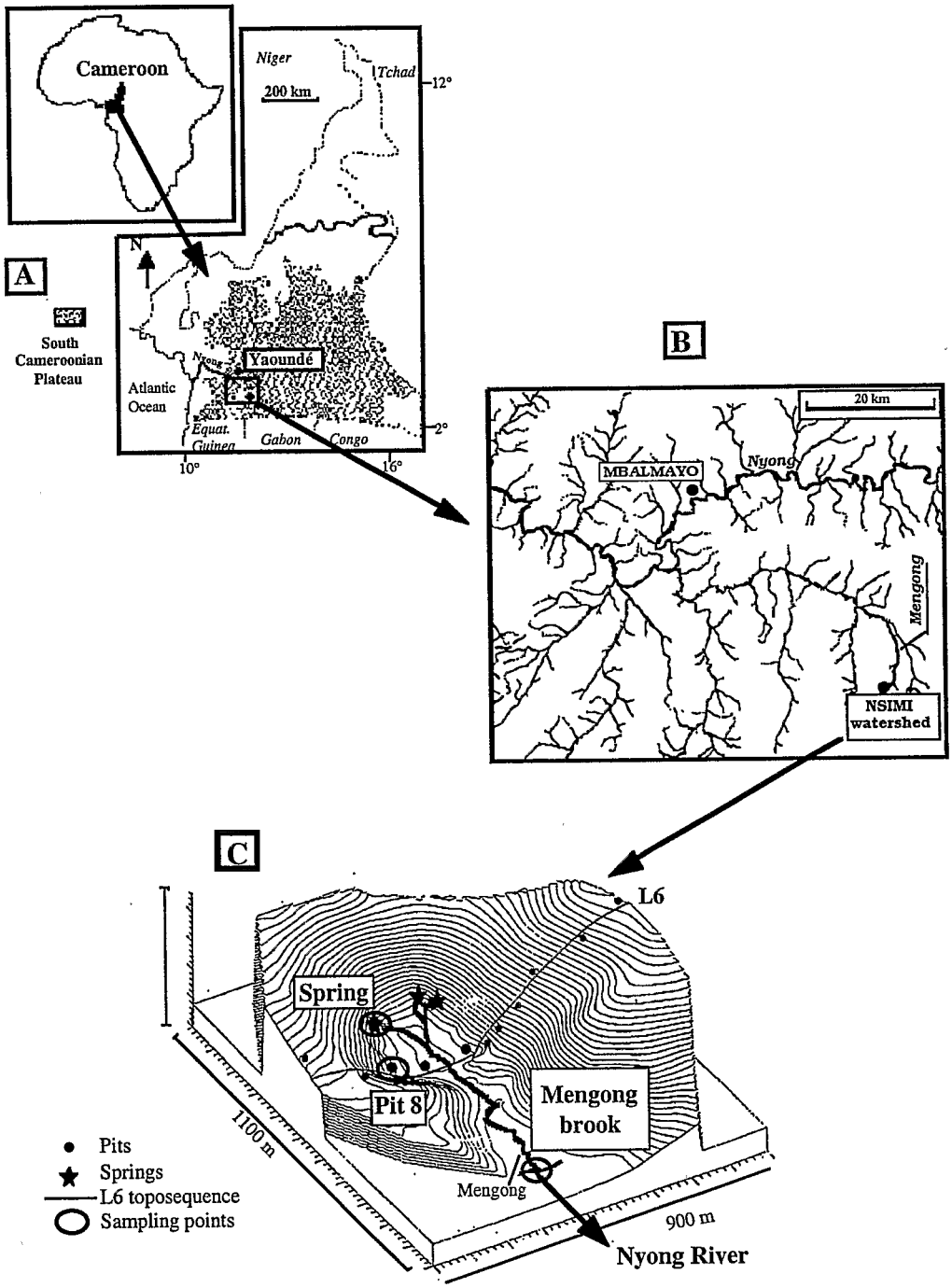

Fig. 1. Geographical location of (A) the Nyong hydrological system and (B) the Nsimi–Zoétélé small watershed. (C) Three-dimensional representation of the Nsimi–Zoétélé site and sampling point localities (pit 8, spring, Mengong brook).

collected at these two sites: one sample of indurated ferruginous materials has been hand-picked at 2 m depth in pit 8; and the second sample of clayey yellow material (topsoil) was taken from the spring

site. Coloured river water has been sampled in the Mengong brook at the exit of the Nsimi–Zoétélé catchment, and in the Nyong river near the town of Mbalmayo, around 50 km from the Nsimi–Zoétélé catchment. The water samples were collected on two days at each site during two hydrologically distinct periods: in May 1995, during the short rainy season (day 1) and in November 1995, during the long rainy season (day 2).

3. Field and laboratory techniques

3.1. Samples: sampling procedure, concentration, chemical composition

Sixty litres of the ground and river water were filtered through 50 μm membranes to cellulose acetate. The filtrate was then ultrafiltered at basecamp at most 3 h after sampling, using a common tangential-flow ultrafiltration scheme (see Eyrolle et al., 1996 and references therein). Four cutoffs have been used: 0.45 and 0.2 μm, and 300 and 20 kDa. Concentration factors ranged between 45 and 130 depending on the solid load in the water samples. In this study, the material recovered in the size fraction ranging from 50 to 0.45 μm is called particulate (P), while material recovered in the smaller size fraction is colloidal, either coarse (C1: 0.45 μm–0.2 μm), medium (C2: 0.2 μm–300 kDa) or fine (C3: 300 kDa–20 kDa). The finest filtrate (< 20 kDa) was considered as the 'soluble' fraction. Retentates obtained after each ultrafiltration step were immediately freeze-dried for spectroscopic analyses. A portion of the unfiltered water and filtrates was prepared for total organic carbon (TOC) analysis by storage in a dark environment at a temperature of 4°C after addition of an antibiotic ($[HgCl_2] < 4 \times 10^{-5}$ M) to prevent bacterial development. Another aliquot of the unfiltered water was acidified (pH ≈ 1) with ultrapure HNO_3 for chemical analysis by ICP-MS (see below).

The total SM content (collected by ultrafiltration) was determined from the cumulative mass of freeze-dried retentates and the initial volume of water. The corresponding data are detailed in Table 1. They correspond to minimum concentrations; as possible loss of material clogging the filter was not taken into account.

The concentrations of Al, Fe, Mn and Si in filtrates were measured by inductively coupled plasma mass spectrometry (Elan 500, Perkin-Elmer ICP-MS) at the Laboratory of Geochemistry (Univ. P. Sabatier; Toulouse, France). TOC was analysed on a Shimadzu carbon analyser (TOC 5000) (CEREGE; Aix-en-Provence, France).

3.2. Mineralogical analyses

X-ray powder diffraction data were obtained with a Philips PW 1729 vertical goniometer using Co Kα radiation (40 kV, 30 mA), two sets of Sollers slits, 1° divergence and scatter slits, a 0.2 mm receiving slit and a graphite back-monochromator. Data were collected from 3° to 70° 2θ, counting for 20 s at every 0.04° 2θ step. Freeze-dried samples were suspended in acetone and deposited on aluminum (SH) or silicon (SH′) plates.

Table 1
Total concentration of collected SM in the water and corresponding percentages of SM in the particulate (> 0.45 μm) and colloidal (< 0.45 μm; > 20 kDa) fractions

		Concentration of SM (mg/l)	Percent particulate fraction	Percent colloidial fraction
SRS	Pit 8	2.097	95	5
	Spring	0.71	85	15
	Mengong	11.2	44	56
	Nyong	20.5	78	22
LRS	Pit	0.32	62.5	37.5
	Spring	0.46	78	22
	Mengong	20.02	60	40
	Nyong	18.15	55	45

FTIR spectra were recorded in transmission mode with a Perkin-Elmer 16PC spectrometer. They were registered in the Mid-IR range (4000–250 cm^{-1}) with a 2 cm^{-1} resolution. About 1.25 mg of gently ground freeze-dried sample was mixed with 500 mg of ground KBr, and pressed in a vacuum die (300 mg, 13 mm in diameter). The presence of sorbed water was decreased by drying the pellets at around 80°C for 48 h. No subsequent change in FTIR spectra of the organic matter was observed; the spectra of samples before and after drying were qualitatively similar, except for two bands at 660 and 2340 cm^{-1}, which can be assigned to a CO_2 artifact (Piccolo and Stevenson, 1982).

EPR measurements were performed at 9.27 GHz (X-band) hyperfrequency using a ESP300E Brucker spectrometer. Both natural and oxidised (see below) freeze-dried samples have been studied by EPR. The EPR spectra were recorded at room temperature within 40–6000 G. The experimental parameters were as follows: 100-kHz modulation frequency, 5.67 G modulation amplitude, 50 mW microwave power, a receiver gain of 8000, and a time constant of 0.16 s. The observed EPR signals were described by their effective g values, g being the EPR spectroscopic factor defined by the relation $h\nu = g\beta H$, where H is the field at which resonance occurs, ν is the resonance frequency, β is the Bohr magneton and h is Planck's constant. The g-values were calibrated by comparison with a standard (DPPH, $g = 2.00037 \pm 0.0002$), with an instrumental error of ± 0.001. Freeze-dried powdered samples filled calibrated silica tubes (suprasil grade). Although the mass of analysed samples varied within the range 3 ± 0.1–10 ± 0.1 mg, all spectra have been normalised to constant weight for comparison. Additional EPR measurements were also performed at 35 GHz (Q-band) at room temperature. In these cases, the experimental parameters were the following: 100 kHz modulation frequency, 1.99 modulation amplitude, 60 mW microwave power, a receiver gain of 5000 and time constant of 0.32 s.

DRS data were collected in the visible range (16,000–25,000 cm^{-1}) at room temperature, using a CARY 2300 spectrophotometer. Measurements were made relative to a Halon standard. The Kubelka–Munk formalism was used to model the absorption of the scattered light in the form of a remission function (e.g., Wendlandt and Hecht, 1966). Noise reduction of the experimental spectra was performed using a Fourier Transform filtering procedure (Brigham, 1988). The absorption band positions were determined by using the minima of the second derivative curve (see Malengreau et al., 1994, for further details), with an estimated error of ± 100 cm^{-1}. With regard to iron oxide analyses, a strong interference arose from the presence of organic matter in samples from the coloured water. This organic matter is responsible for a broad absorption band superimposed on the iron oxides bands in the visible range. Consequently, organic matter was removed from an aliquot of the freeze-dried samples using a sodium hypochlorite oxidative treatment at room temperature. After 12 h, the remaining mineral phases were removed by centrifugation, and then washed with distilled water and dried at room temperature.

TEM of selected samples were performed with a Philips EM 420 equipped with an energy dispersive spectrometer, which allowed quantitative in-situ microanalyses. The grids (collodion-coated and carbon-coated) were prepared in the field according to the procedure of Perret et al. (1994) in which unfiltered water is embedded in a hydrophilic resin (Nanoplast) and coated on grids using a horizontal microcentrifuge.

4. Results

4.1. Concentration of SM and chemical analysis

The concentration of SM is much lower in colourless water than in coloured water, irrespective of the sampling day (Table 1). In colourless water, the SM content is around 1–2 mg/l (day 1), and decreases to below 0.5 mg/l on day 2 due to a dilution effect. In both cases, a major part of SM (more than 60%) occurs in particulate fraction. In comparison, except for the Nyong water collected at day 1, the colloidal fraction contributes 40% to 56% to the SM content of the coloured water. Regardless of the sampling day, the SM content of the coloured water ranges between 10 and 20 mg/l, i.e., at least twice that of colourless water.

The main chemical properties of the water collected on day 2 are presented in Table 2. Unfortu-

Table 2
Al, Si, Fe, Mn and TOC concentrations in the filtrates collected on day 2 by tangential ultrafiltration

		Sampling sites			
		Pit 8	Spring	Mengong	Nyong (Mbalmayo)
Al (μmol/l)	< 0.2 μm	0.12	0.37	3.35	4.37
	< 300 kDa	0.23	0.20	2.54	0.95
	< 20 kDa	0.30	0.28	3.4	0.78
Si (μmol/l)	< 0.2 μm	158.3	120	190	178.3
	< 300 kDa	165	131.6	195	181.6
	< 20 kDa	158.3	133	196.6	181.6
Fe (μmol/l)	< 0.2 μm	0.41	0.05	1.53	2.9
	< 300 kDa	0.51	0.05	1.18	0.32
	< 20 kDa	0.61	0.02	1.13	0.21
Mn (μmol/l)	< 0.2 μm	0.07	0.09	0.11	0.60
	< 300 kDa	0.07	0.10	0.07	0.17
	< 20 kDa	0.06	0.10	0.1	0.21
TOC (ppm)	Unfiltered water	0.9	0.83	12.5	11.2
	< 0.2 μm	–	–	9.6	7.35
	< 300 kDa	–	–	7.7	5.95
	< 20 kDa	–	–	6	4.25
pH	Unfiltered water	4.8	4.85	5.3	5.9

nately, it was not possible to determine concentrations in unfiltered water. Coloured water (< 0.2 μm) is characterised by much higher concentrations of TOC, Al, Fe, Si and Mn than colourless water. In particular, Fe and TOC concentrations are one order of magnitude higher. Water from the river system (Mengong, Nyong) is weakly acidic (pH = 5.3 to 5.9) and contains high amounts of organic substances (TOC = 7 to 10 mg/l). Similar properties were found for water collected on day 1 (see Viers et al., 1997 for the details). This coloured water is similar to some "black river" systems from Amazon and Congo basins (Berner and Berner, 1987; Dupré et al., 1996).

The effect of successive filtrations (300 and 20 kDa) on the elements concentrations (Table 2) provides information on the element distribution in the water collected on day 2. In the colourless water, the Si and Mn concentrations remain unaffected by reducing pore size down to 20 kDa. In contrast, the Fe and Al concentration decreases for spring water. Because of the slight increase of Fe and Al concentrations by filtration in the pit 8 samples, the distribution of these elements has not been investigated in the pit 8 water. As the concentration of TOC is very low (< 1 mg/l) and the analytical uncertainties are comparatively large (around 0.5 mg/l), we could not detect any change in its concentration as a result of filtration. The above results show that only Al and Fe are present in the colloidal fractions in the spring water, whereas Si and Mn are dissolved or associated with colloids smaller than 20 kDa in the pit 8 and spring waters. In comparison with the colourless water, in the coloured water, the Al, Fe, Mn and TOC concentrations are strongly and continuously decreased by the successive filtrations, indicating that these elements are essential components of solid river-borne materials. As in colourless water, Si is not affected by filtration; its concentration remains almost constant in all filtrates.

These results are in agreement with those of Viers et al. (1997) obtained on day 1. We conclude that in many cases, particularly in coloured water, the filtration experiments indicate that colloids play an important role on the speciation of Al, Fe, Mn, and TOC.

4.2. X-ray powder diffraction

Representative XRD patterns of SM collected on day 1 are presented in Fig. 2A and B, for the spring and the Mengong brook, respectively. (Note that for

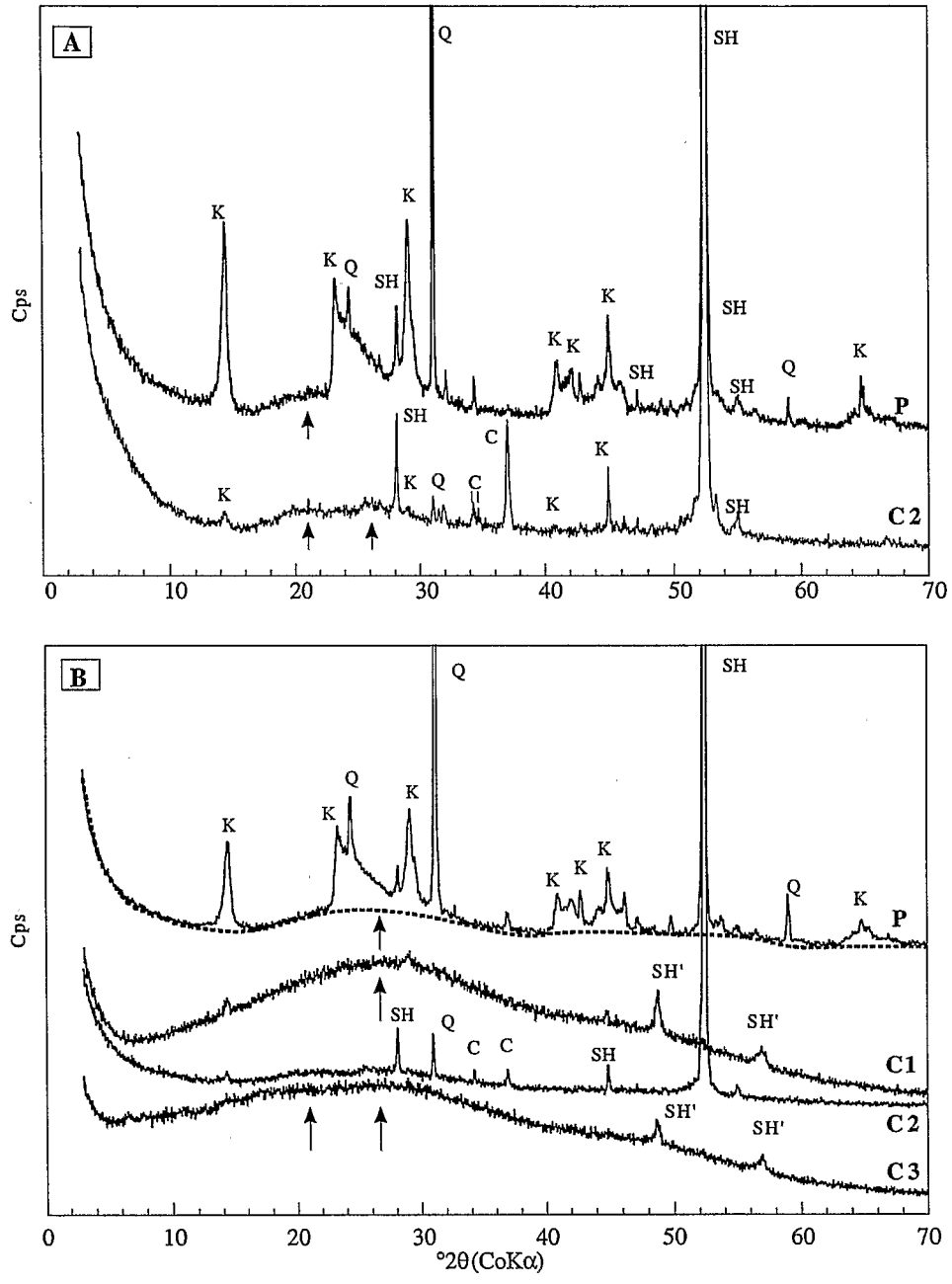

Fig. 2. Selected X-ray powder diffraction patterns of suspended matter collected during the short rainy season (day 1). (A) fractions derived from the colourless water at the spring site, (B) fractions derived from the coloured water at Mengong brook. ($P > 0.45$ μm; 0.45 μm > C1 > 0.2 μm; 0.2 μm > C2 > 300 kDa; 300 kDa > C3 > 20 kDa). K = kaolinite; Q = quartz; C = carbonates; SH and SH′ = sample holders; ––– = background.

the samples collected on day 2, the XRD patterns (not shown) of both particulate and colloidal fractions were found to be similar to samples from day 1.)

The XRD patterns of the particulate fractions from day 1 at the different sampling sites show similar features. In both Fig. 2A and B, XRD profiles for quartz and for kaolinite are superimposed. In addition to the marked 001 ($d = 7.15$ Å or 14.3° 2θ) and 002 ($d = 3.6$ Å or 28.7° 2θ) reflections, the XRD profile for kaolinite clearly exhibits the 02.11 and 20.13 bands [22° to 28° ($d = 4.7$ to 3.7 Å) and 40° to 46° ($d = 2.6$ to 2.3 Å) 2θ, respectively], which are characteristics of disordered kaolinites (Brindley, 1980). These minerals are also present in all the soil materials collected. Broad (10° to 40° 2θ), weak scattering bands are also present on the XRD patterns at about 21° and 26° 2θ. These bands are indicative of the presence of amorphous phases, and are particularly apparent in the samples from coloured water, where the relative intensities are much more pronounced. The main scattering band located near 26° 2θ ($d = 4$ Å) may be attributed to amorphous silica (Graetsch et al., 1994). Nevertheless, a contribution due to organic matter cannot be excluded (Kodama and Schnitzer, 1967).

The XRD patterns of colloidal fractions differ from those of the particulate fractions described above. They are mostly dominated by broad, sometimes intense bands due to amorphous phases (Fig. 2A and B). Although weak, the main characteristic reflections of kaolinite and quartz are also observed. Two additional peaks at about 34° and 37° 2θ ($d = 3$ and 2.8 Å) are attributed to carbonates, which are most likely artifacts of the drying procedure used (Hart et al., 1993).

4.3. FTIR spectroscopy

FTIR absorption spectra of SM collected on day 1 from the spring and the Mengong brook are presented in Fig. 3; their spectra are representative of the colourless and coloured water, respectively. Three main groups of absorption bands are observed: those located in the 250–1200 cm^{-1} and 3500–3800 cm^{-1} regions are mainly due to mineral phases, whereas those observed in the 1200–3500 cm^{-1} region are due to organic components. In addition, the large band at around 3430 cm^{-1} and the band near 1630 cm^{-1} arise from stretching and bending vibrations of water molecules adsorbed on the sample surfaces.

4.3.1. Mineral phases

FTIR spectra of the particulate fractions exhibit similar absorption bands, irrespective of the sampling site and period. Most bands are characteristic of kaolinite (Farmer and Palmieri, 1975). Expanded spectra of the OH-stretching bands (3800–3500 cm^{-1}, not shown) show that the band at 3649 cm^{-1} is significantly more intense than that at 3669 cm^{-1}. This is ascribed to structural disorder of kaolinite (Cases et al., 1982), in good agreement with the XRD data. Two weak bands at around 397 and 368 cm^{-1} are due to SiO vibrations in quartz, the other bands being superimposed on those of kaolinite in the region 300–1100 cm^{-1}.

FTIR spectra of the colloidal fractions (Fig. 3A and B) differ from that of the particulate fraction. In addition, they strongly depend on the sampling sites. The three main broad bands located near 470, 800 and 1100 cm^{-1} are a common feature in the FTIR spectra of colloids separated from colourless water. The positions of these bands are characteristic of polymerised SiO_2, such as opal (Graetsch et al., 1994). Such bands are also present, although weak, in the colloid spectra from coloured water. However, they cannot be unambiguously attributed only to amorphous silica, because they have also been observed with similar relative intensities in the FTIR spectra of humic or fulvic substances (Vinkler et al, 1976; Leenheer and Noyes, 1989). Although very weak, the main diagnostic bands for kaolinite, at 1035, 540 and 3690, 3620 cm^{-1}, are still visible in the FTIR spectra of the colloidal fractions larger than 300 kDa, particularly from the colourless water. In addition to the bands described above, the spectra of the colloids from the colourless water include three sharp 1400, 875 and 700 cm^{-1} bands which are ascribed to a minor carbonate phase (interpreted as a preparation artifact; see XRD section).

4.3.2. Organic matter

The spectra in Fig. 3A and B imply that organic components are present in all size fractions. As expected, they are particularly abundant in the SM from the coloured water (Fig. 3B). The corresponding spectra resemble the spectra previously reported from similar systems (e.g., Beck et al., 1974; Alberts et al., 1976). The main FTIR bands are assigned

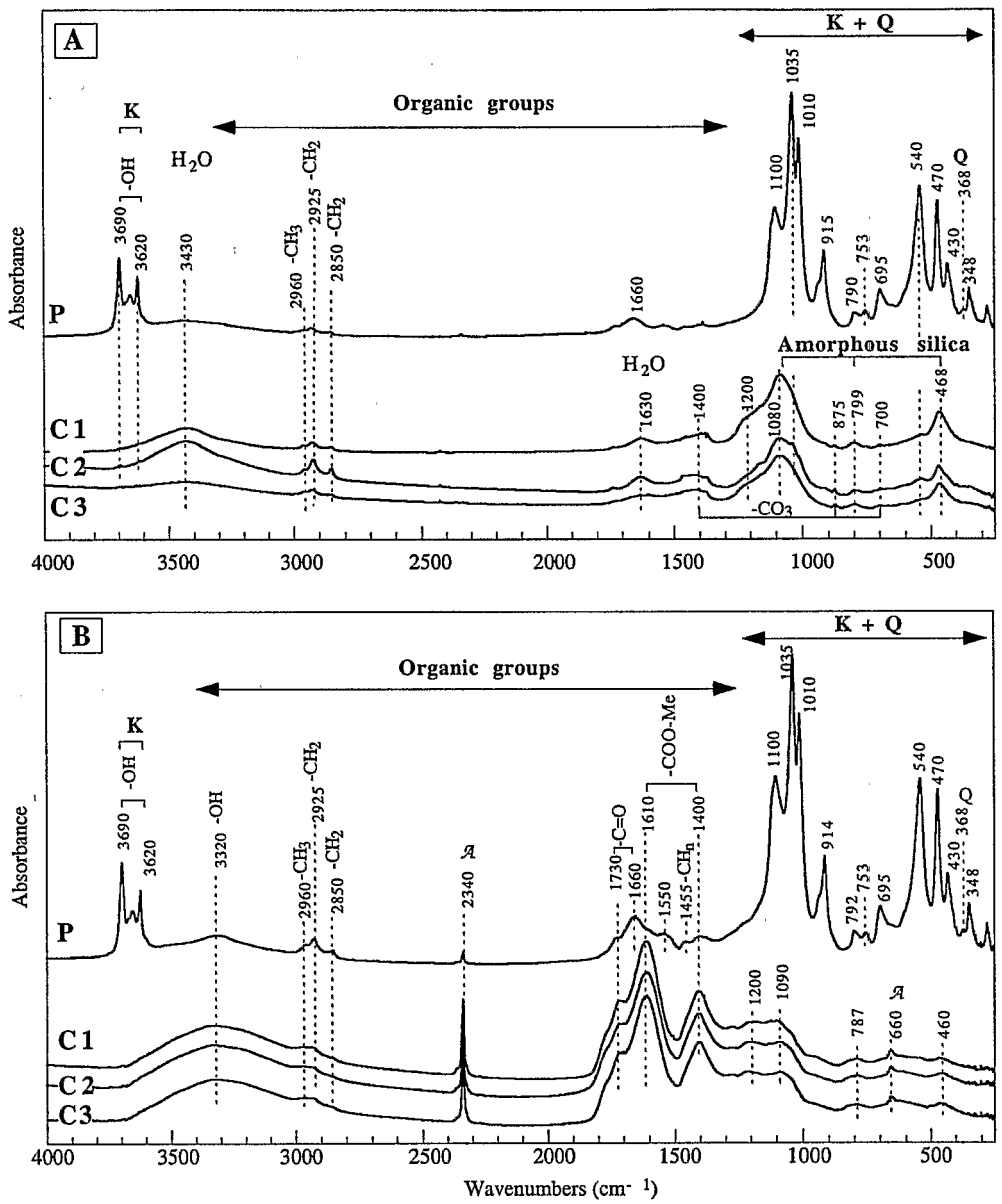

Fig. 3. Selected FTIR spectra in the range 250–4000 cm^{-1} for particulate and colloidal fractions of suspended matter collected during the short rainy season (day 1): (A) fractions derived from the colourless water at the spring site; (B) fractions derived from the coloured water at Mengong brook. ($P > 0.45$ μm; 0.45 μm > C1 > 0.2 μm; 0.2 μm > C2 > 300 kDa; 300 kDa > C3 > 20 kDa). K = kaolinite; Q = quartz; ⁂ = preparaton artefact (see text).

according to Stevenson and Goh (1971) and Gerasimowicz et al. (1986). In the particulate fraction, the most intense contributions consist of: a triplet at around 2850–2960 cm^{-1} arising from stretching of CH_2, CH_3 groups and band at 1455 cm^{-1} due to CH_n groups; a doublet at 1660–1730 cm^{-1} interpreted as mainly arising from C=O bonds; and a band at 1550 cm^{-1} consistent with NH deformation

or carboxylate stretching. The spectra of colloids from the coloured water (Fig. 3B) clearly present new features. A rather strong and broad band occurs at 3320 cm^{-1}. The position of this absorption band is shifted about 100 cm^{-1} toward low wavenumbers with respect to OH of organic groups as phenolic, alcoholic, carboxylic groups. This shift is expected to occur when organic groups are involved in metal bonding, to an extent which depends on the nature of the bonded metal (Senesi, 1992 and references therein). Moreover, the position of this band is close to that measured at 3325 cm^{-1} for humic acid complexes with iron (Banerjee and Mukherjee, 1972). Two intense absorption bands are also consistently observed at 1610 and 1400 cm^{-1}. Their presence is tentatively explained according to the experimental works of Piccolo and Stevenson (1982) and Senesi (1992). These authors demonstrated that addition of metals, such as Fe, Cu or Pb, to natural organic acids causes a significant increase in the intensity of the peaks near 1600 and 1400 cm^{-1}. Therefore, these results strongly suggest the presence of carboxylate-metal complexes among the colloidal organic matter from the coloured water.

The spectra of the SM from the colourless water show a minor contribution due to organic matter. Only a few weak absorption bands, arising from stretching of CH_2 and CH_3 groups, are clearly observed (Fig. 3A).

In summary, the FTIR analysis of SM is fully complementary to XRD analysis, as it provides detailed information about the nature of amorphous phases of organic as well as inorganic composition. In each geochemical system (colourless and coloured water), all colloidal fractions show similar compositions irrespective of size fraction. Moreover, no significant difference in the nature of the SM components was observed as a function of sampling season. However, except for pit 8, the particulate fractions collected on day 2 showed a strong decrease in the proportion of crystalline phases (kaolinite and quartz) relative to amorphous phases (opal or organic matter).

4.4. EPR spectroscopy

Selected EPR spectra are presented in Fig. 4A for representative samples of the soil material (Pit 8),

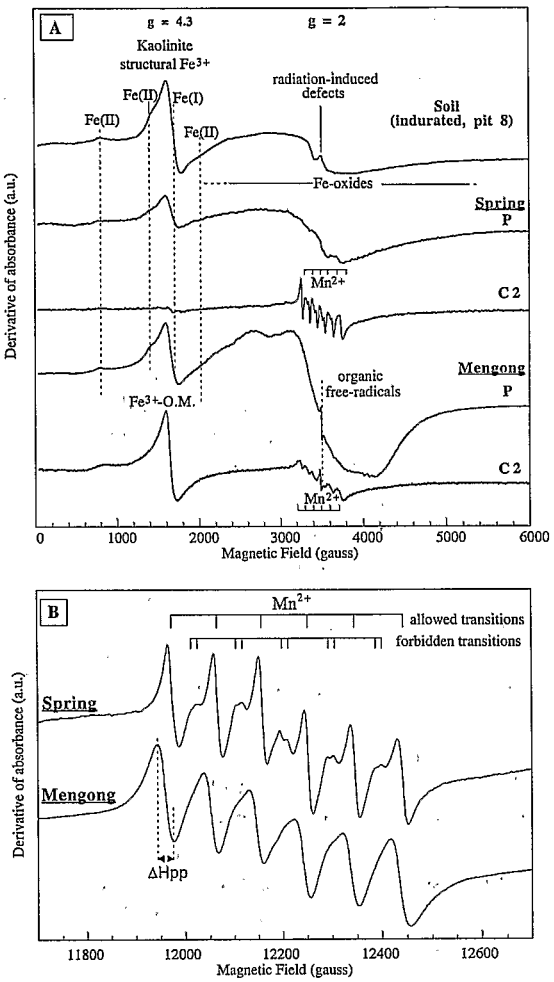

Fig. 4. (A) Typical full range X-band EPR spectra of indurated soil material (pit 8) and of suspended matter from the spring and Mengong, collected during the short rainy season (day 1). (B) Q-band spectra of Mn^{2+} in colloidal fractions (C2) derived from the spring and Mengong brook. ($P > 0.45$ μm; 0.2 μm > C2 > 300 kDa).

colourless water (spring) and coloured water (Mengong brook). The nature and relative amounts of these various paramagnetic species make it possible to distinguish between the particulate and colloidal fractions, as well as between the two hydrological systems.

Particulate fractions sampled on day 1 exhibit EPR spectra very similar to that of the soil materials, irrespective of the sampling site (Fig. 4A). They exhibit most of the resonances which have been

described for lateritic soil kaolinites (e.g., Muller and Calas, 1993b). At low magnetic field, several resonances are observed around $g = 4.3$, which unambiguously arise from Fe^{3+} ions substituting for Al^{3+} within the kaolinite structure. Two distinct spectra are identified and referred to as Fe(I) and Fe(II), in relation to local crystallographic order around Fe^{3+}. In the studied samples, the prevalence of the Fe(I) signal over that of Fe(II) is characteristic of disordered kaolinite, which is in full agreement with XRD and FTIR results. Furthermore, kaolinite from the soil, spring and Mengong brook particulate fractions have very similar EPR signatures, indicative of similar formation conditions. The broad isotropic resonance ($\Delta H > 1000$ G) centered at $g = 2$ (around 3500 G) is primarily caused by superparamagnetic iron oxides which are naturally associated with kaolinite, either as inclusions or coatings (Malengreau et al., 1994). The contribution of these phases is most significant in the particulate fractions from the coloured water. The narrow and weak signal superimposed on that of the iron oxides at $g = 2$ arises from radiation-induced defects, present in kaolinites from any environment (Clozel et al., 1994).

The colloidal fractions exhibit very different EPR spectra from the particulate fractions (Fig. 4A). In the $g = 4.3$ region, no significant signal is observed for colourless water colloids. In contrast, the coloured water colloids all exhibit an intense and specific signal which has been shown to result from Fe^{3+} ions complexed with organic groups (Olivié-Lauquet et al., 1999). This result is in agreement with the interpretation of FTIR spectra, considering occurrence of metal-organic matter complexes primarily in colloidal fractions from the coloured water. In these latter samples, the EPR spectra consistently exhibit an additional sharp resonance (a few Gauss width) at $g = 2.004$, which arises from stable organic free radicals, as is commonly observed in humic substances (Cheshire and Senesi, 1998).

A common feature of the colloidal fraction spectra is the presence of a six-line signal centered at $g = 2$, which is characteristic of hyperfine structure of Mn^{2+} ions (Muller and Calas, 1993a). Q-band spectra differentiate the colourless from the coloured water systems (Fig. 4B). In colourless water colloids, the Mn^{2+} spectrum exhibits two sets of allowed (intense) and forbidden (weak) resonances, with a hyperfine constant $A = 93$ G. These data are indicative of a crystal/ligand field of low symmetry, and strongly suggest that Mn^{2+} is hosted in a crystalline phase, such as a carbonate phase (Bourghriet et al., 1992). This interpretation is supported by the carbonate contribution on corresponding XRD patterns and FTIR spectra. In contrast, the hyperfine structure of Mn^{2+} in the river colloids is broader; it appears mainly isotropic and does not exhibit forbidden transitions. The very low anisotropy of the six lines ($30 \text{ G} < \Delta H_{pp} < 37$ G) and the value of the hyperfine constant ($A \approx 96$ G) further suggest that Mn^{2+} is weakly bound as $[\,Mn(H_2O)_6]^{2+}$ outer-sphere complexes to organic hydrous surfaces (McBride, 1982; Carpenter, 1983). This is supported by the disappearance of the Mn^{2+} signal after oxidative (NaOCl) and dehydration (100°C heating) treatments (Olivié-Lauquet, 1996), and by the correlation between Mn and TOC content during filtration (see Section 4.1). By reference to Muller and Calas (1993a), the concentration of Mn^{2+} associated with organic matter in the SM was estimated to be near the 100 ppm level, which represents less than half of the total Mn.

The EPR analysis of samples collected on day 2 showed the presence of the same species as on day 1, although with different relative amounts. In accordance with FTIR results, a decrease of the kaolinite contribution (structural Fe^{3+} ...) was observed from EPR in all particulate fractions. Moreover, all fractions from the coloured water, including the particulate fraction, were also dominated by organic complexes.

4.5. Visible DRS

DRS has been performed on the fractions from which enough (i.e., at least 5 mg) material was available. Representative second derivative curves for SM (pit 8, Nyong) and soil materials (pit 8, spring soil) are presented in Fig. 5A and B, respectively. Reference spectra given by Malengreau et al. (1994) and Scheinost et al. (1998) have been used for Fe and Ti oxides identification.

The spectra of the particulate fractions from the colourless water (Fig. 5A) exhibits two main bands located at about 24,100 and 20,660 cm^{-1}, which are

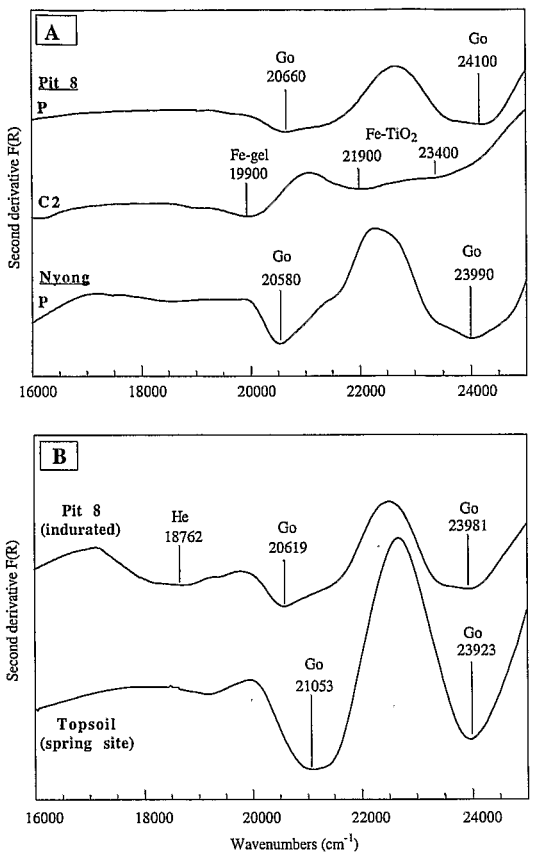

Fig. 5. Selected second derivative curves in the visible region of suspended matter collected during the short rainy season (day 1) (A) at pit 8 and Nyong sites; and (B) soils materials. ($P > 0.45$ μm; 0.2 μm > C2 > 300 kDa).

due to iron oxihydroxides. According to the intensity and the position of these bands, they may be attributed to goethite. Colloidal fractions exhibit drastically different spectra with three distinct weak bands (Fig. 5A); the band located near 19,900 is attributed to ferric gels (ferrihydrite or Fe polymers), whereas the bands around 21,900 and 23,400 cm^{-1} may be attributed to Fe-bearing anatase. The spectrum of the particulate fraction from the Nyong river (Fig. 5A) exhibits two main bands located at about 23,990 cm^{-1} and 20,580 cm^{-1} which, like that of the particulate fraction of the colourless water, may be attributed to goethite.

These DRS results are compared to those of the hardcap materials from pit 8 and the topsoil of the spring site (Fig. 5B). The spectrum of the pit 8 sample exhibits two distinct bands at about 23,980 and 20,620 cm^{-1} and a weak one at 18,760 cm^{-1}. The first are diagnostic bands for goethite while the latter is attributed to hematite. In contrast, the spectrum of the topsoil material at the spring site is characterised by two marked diagnostic bands at about 23,920 and 21,050 cm^{-1}, indicative of goethite (Fig. 5B). Hence, the particulate fractions of SM is characterised by absence of hematite and presence of goethite with DRS spectrum similar to that measured in the indurated materials. None of the colloidal phases collected in the groundwater, i.e., ferric gels and Fe-bearing anatase, could be detected in the soil materials studied, which may be due to the low amount of such phases in the bulk soil samples. However, the formation of such phases is expected at particular levels, such as, for example, in the watertable oscillating zone.

4.6. TEM and optical microscopy observations

Only a few particles were observed in the colourless water. These consisted primarily of kaolinite platelets of a range of sizes, represented in all size fractions. Nevertheless, different morphologies could be discerned in that: the largest particles (> 0.2 μm) typically, exhibited rounded shapes, whereas the smaller ones (typically some 10 nm in size), were mainly hexagonal (Fig. 6A). Aggregates of iron oxyhydroxides are commonly intimately associated with kaolinite particles (Fig. 6A). These observations are in keeping with the previous FTIR and DRS data which revealed traces of kaolinite and iron oxyhydroxides within all size fractions.

In contrast, numerous mineral particles and aggregates of organic matter were observed in coloured water. Mineral phases in the particulate fractions consist of kaolinite particles, quartz grains and biogenic particles of several microns in size. In fact, a unique feature of the river water is the presence of diatom tests and phytoliths with various shapes (Fig. 6B). These particles (composed of opal) explain the amorphous pattern observed by XRD on particulate fractions. However, this observation could not be confirmed by FTIR, owing to the predominance of

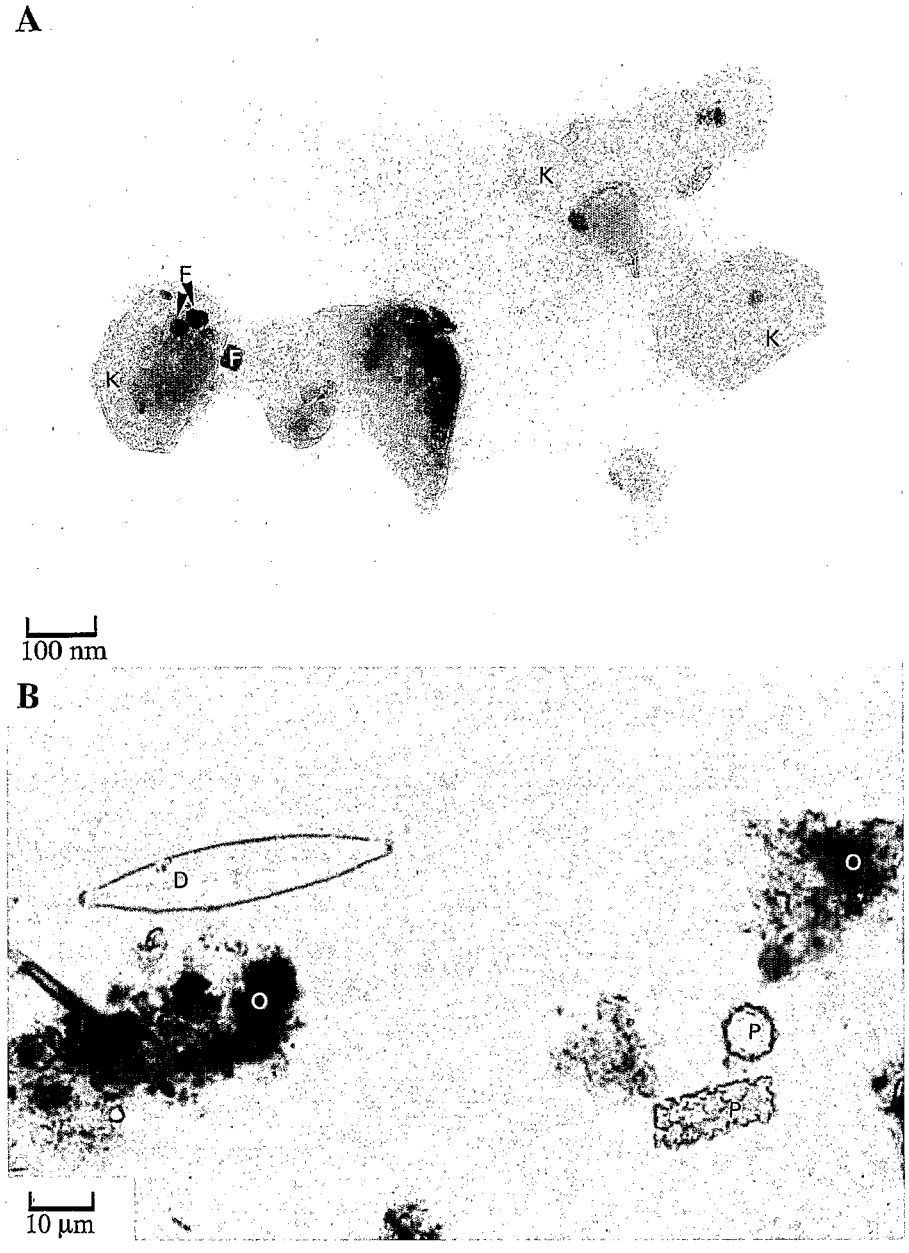

Fig. 6. (A) Transmission electron micrograph of suspended matter from the spring site (K = kaolinite; F = iron oxyhydroxide). (B) Optical micrograph of particulate fraction from Mengong site (D = diatom frustule; O = organic matter; P = phytolith).

the kaolinite signal. The colloidal fraction in coloured water was dominated by the presence of organic aggregates which precluded identification of mineral phases. Thus, occurrence of colloidal kaolinites could not be confirmed by TEM observations in these samples.

5. Discussion

5.1. Speciation of Al, Si, Fe, Mn

The phases and chemical species identified in the present study from colourless and coloured water sampled on day 1 are summarised in Fig. 7. They are discussed below element by element , and compared with the phases predicted by the thermodynamic calculations of Viers et al. (1997).

The only major Al-bearing phase, which could be unambiguously identified, is kaolinite, which is concentrated in the particulate fractions. In many cases, traces of kaolinite could also be detected in colloidal fractions of both clear and coloured water. Several geochemical studies of lateritic soil or river systems concluded that the concentration of dissolved Al is controlled by equilibrium with kaolinite (Sarazin et al.,1982; Nkounkou and Probst, 1987; Lucas et al., 1996). In the clear water, the presence of small euhedral kaolinite particles in the colloidal fractions is thus in agreement with the results of Viers et al (1997). However, the presence of colloidal kaolinite in the coloured water was not predicted by these authors, as they indicated that most Al should be complexed with organic matter.

In addition to Al, Si is also a constituent of kaolinite. However, the Si concentration in the water is so high relative to Al that the proportion of Si constituting kaolinite is negligible (< 3%) (Viers et al, 1997). In the particulate fraction, Si is then mainly in biogenic opal and/or quartz. In the colloidal fractions of clear water, FTIR analysis provided evidence for amorphous silica, although chem-

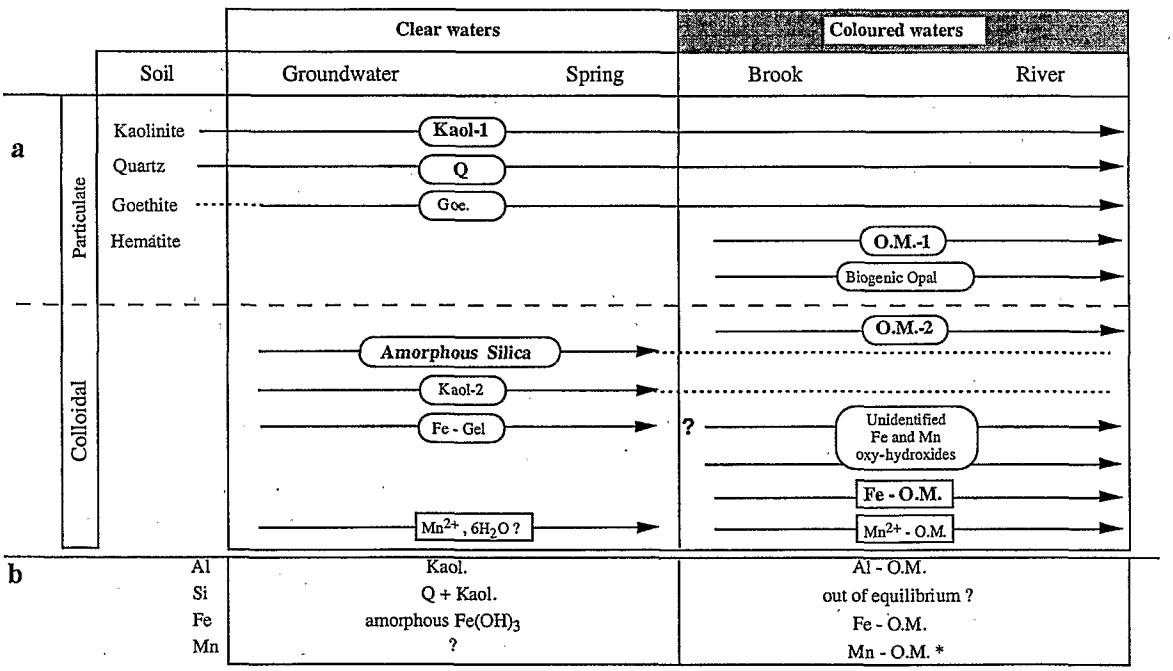

Fig. 7. Summary of studied Al, Si, Fe and, Mn transport as suspended matter in the Nyong basin. (a) Phases (rounded boxes) and species (square boxes) determined in freeze-dried samples (this study) are either particulate (50 to 0.45 μm) or colloidal (0.45 μm to 20 kDa). Major components are in bold characters, minor ones in plain, small characters. Plain arrows indicate continuity in crystal chemical characteristics of phases and species, supporting inheritance during transport. Starting of arrows in hydrological system strongly suggests in situ formation. Dashed lines indicate unconfirmed existence of the phase. (b) Phases or complexes controlling concentrations of Al, Si, Fe, Mn in < 0.2 μm filtrates (after Viers et al., 1997): according to thermodynamic calculations when not specified, or suggested by correlations of concentrations in the various filtrates (*). Comparison of (a) and (b) evidences that mineralogical results give direct confirmation of previous geochemical results. Most of expected phases and species are observed in the colloidal fraction, except for opal which may have been artificially precipitated (see text for details).

ical analyses showed that Si was mainly concentrated in the 'soluble' fraction. Two interpretations can account for these results. First, Si could be present as colloids with sizes below 20 kDa, or even 5 kDa, according to chemical analyses of Viers et al. (1997). Second, Si could be present in 'true dissolved form', i.e., H_4SiO_4, then precipitate from solution during freeze-drying of retentates. In addition to these assumptions, the possible occurrence of colloidal silica in coloured water could result from the disaggregation of phytoliths and diatoms, which have a substructure of extremely small particles less than 5 nm in diameter (Iler, 1979).

At Nsimi–Zoétélé catchment, Fe-bearing phases are identified in all fractions and consist mainly of iron oxides in the whole hydrosystem and organic matter in the coloured water. In the clear water, the presence of ferric gels in the colloidal fraction is in full agreement with the geochemical interpretation of Viers et al. (1997). In Nyong and Mengong, the direct observation by EPR of iron oxyhydroxides and iron organic complexes is consistent with the geochemical results obtained by Eyrolle et al. (1996) in coloured water from a small tropical catchment (Brazil). In particular, it has been recently shown that the Fe^{3+} oxyhydroxides contribute significantly (more than 30%) to iron transport in the coloured water system (Olivié-Lauquet et al., 1999). The previously held view that only metal-humate complexes can control iron concentration in this system appears oversimplified (Viers et al., 1997). The occurrence of colloidal iron oxyhydroxides is emphasised since these phases are also expected to have large sorption capacities for numerous trace elements (Johnson, 1986; Tessier et al., 1996).

In clear water, Mn is found in the 'soluble' fraction by chemical analysis. Moreover, Mn^{2+} occurs in colloidal carbonates that were likely introduced as an artifact of sample preparation. This indicates that some Mn was present in clear water in its lower redox state. In river colloids, some of the Mn is directly determined to be complexed with organic matter in the Mn^{2+} redox state, which confirms the previous assumption by Viers et al. (1997). The presence of reduced Mn^{2+} species has previously been indicated in soil organics and river water (e.g., McBride, 1982; Laxen et al., 1984). Nevertheless, it is assessed in this study that a significant part of Mn may be present in a higher redox state, possibly as insoluble Mn^{3+}–Mn^{4+} oxyhydroxides (De Vitre and Davison, 1993) and/or Mn^{3+} organic complexes (Kostka et al, 1995).

5.2. Origin of transported phases

Knowing the crystal chemistry of SM permits the discussion of the origin of mineral solids transported into the hydrosystem (Fig. 7). The mineralogical composition of the particulate fractions is monotonous in the whole hydrosystem, and consists mainly of kaolinite, quartz and goethite. The spectral signatures of kaolinite and goethite mimic those determined on materials from upper horizons of the laterite (e.g., pit 8). Indeed, according to FTIR and EPR, kaolinite shows similar high degrees of disorder both in the soil-derived materials and in the hydrosystem. In contrast, materials from deeper horizons, sampled in soils upslope of the toposequence and from spring topsoil have different signatures from those of particulate SM; kaolinite from deeper horizons (not shown) and goethite from spring topsoil shows lower degrees of disorder (Olivié-Lauquet, 1996) and different DRS spectra, respectively. Thus, these results suggest inheritance of particulate SM from selected parts of the soil toposequence, in particular, upper horizons drained by the clear water. In contrast, biogenic opal particles are only detected in coloured water. These particles are mainly inherited from the hydrographical system: diatoms are produced in situ and phytoliths are likely to originate from vegetation in the swampy zone, such as palm trees (Piperno, 1987). Such biogenic particles have been shown to contribute significantly to the Si content of river in tropical regions (Giresse et al., 1990). In contrast to the particulate fractions, the presence of colloidal kaolinite platelets (labelled ''kaol2'' in Fig. 7) and ferric gels suggest a recent formation in the groundwater. This interpretation is supported by thermodynamic equilibrium calculations (Viers et al, 1997). Both mineral and organic colloidal matter transported out of the Nsimi–Zoétélé catchment mainly originate from the swampy zone, because of the low concentration of matter in clear water.

Similar phases were observed in the samples irrespective of the sampling season. However, an in-

creased contribution of organic matter in the particulate fraction of coloured water on day 2 was observed as a result of increased mechanical erosion of the swampy zone. Despite the important role of organic matter in iron transport in coloured water, the proportion of iron transported as oxyhydroxides is significantly higher in Nyong than in Mengong (Olivié-Lauquet et al., 1999). This suggests a contribution of mechanical erosion to the solid load of Nyong river basin corresponding to areas where mineral particles prevail over organic compounds.

6. Conclusion

The use of several complementary techniques, including solid-state spectroscopies, allows the determination of the nature of particulate and colloidal SM, whether organic or inorganic, in a tropical hydrosystem. The nature of these phases is strongly dependent on their particle size and their origin in the two subsystems considered, i.e., clear water vs. coloured water. The suspended load of clear water is low (< 3 mg/l) and mostly contains mineral phases, such as poorly ordered kaolinite, plus quartz and goethite in the particulate fraction; and euhedral kaolinite plus amorphous iron oxyhydroxides in the colloidal fraction. In contrast, the coloured water has larger particle loads (at least 10–20 mg/l) and are organic-rich, particularly in the colloidal fraction. Apart from organic matter and biogenic opal, the particulate fraction in coloured water contains the same mineral phases as in clear water. In the colloidal fraction, organic matter dominates and direct evidence of Fe^{3+}- and Mn^{2+}-organic complexes is shown by EPR spectroscopy.

Most phases and species identified in the colloidal fraction confirmed the expectations from thermodynamic equilibrium calculations by Viers et al. (1997) to explain Al, Fe, Mn (and some Si) solubilities. Additionally, in coloured water, EPR results show that colloidal Fe-oxyhydroxides are omnipresent and should therefore be considered as part of the mechanisms of element transport.

The crystal chemical analysis of SM in the hydrosystem can be used to specify its origin. The nature of crystalline mineral phases in particulate fractions is similar to that of particular soil areas adjacent to the river, indicating that inheritance and mechanical erosion processes dominate. In contrast, the colloidal fractions are more influenced by their origin from either of the two geochemical systems: phases formed either in groundwater (e.g., recently formed Fe gels) or in the swampy zone (e.g., organic matter). Organic matter, which promotes mineral alteration and chemical erosion, is shown to play important role in the transport of trace elements, such as Fe and Mn.

Acknowledgements

This work was supported by the French program Programme Environment Géosphère Intertropicale (PEGI) jointly funded by the INSU/CNRS and ORSTOM Institutes. Jean-Jacques Braun, Jules Ndam and Jean-Pierre Bedimo Bedimo are acknowledged for their assistance during the sampling. We thank Bernard Dupré and Jérome Viers for supplying the ICP-MS analysis. We would also like to acknowledge Astrid Vilge and Thierry Boulangé for their support in the TOC analyses. Anne-Marie Jouannet is thanked for analytical assistance during the TEM observations. B.T. Hart and one anonymous reviewer are acknowledged for their constructive remarks.

References

Alberts, J.J., Schindler, J.E., Nutter, D.E., Davis, E., 1976. Elemental, infra-red spectrophotometric and electron spin resonance investigations of non-chemically isolated humic material. Geochim. Cosmochim. Acta 40, 369–372.

Banerjee, S.K., Mukherjee, S.K., 1972. Studies of the infrared spectra of some divalent transitional metal humate. J. Indian Soc. Soil Sci. 20, 91–94.

Beck, K.C., Reuter, J.H., Perdue, E.M., 1974. Organic and inorganic geochemistry of some coastal plain rivers of the southeastern United States. Geochim. Cosmochim. Acta 38, 341–364.

Berner, E.K., Berner, R.A., 1987. The Global Water Cycle. Prentice-Hall, Englewood Cliffs, NJ, 397 pp.

Bessoles, B., 1980. Géologie de l'Afrique, vol. 2: La chaîne panafricaine, zone mobile d'Afrique centrale et zone mobile soudanaise. Mémoires du BRGM 92, 398 pp.

Bourghriet, A., Ouddane, B., Fisher, J.C., Wartel, M., Leman, G., 1992. Variability of dissolved Mn and Zn in the Seine estuary and chemical speciation of these metals in suspended matter. Water Res. 26, 1359–1378.

Brigham, E.O., 1988. The Fast Fourier Transform and Its Applications. Prentice-Hall, Englewood Cliffs, NJ.

Brindley, G.W., 1980. Order–disorder in clay mineral structures. In: Brown, G.W., Brindley, G.W. (Eds.), Crystal Structures of Clay Minerals and Their X-Ray Identification. Mineralogical Society, London, pp. 125–195.

Buffle, J., Van Leuwen, H.P, 1992. Environmental Particles 1. Environmental Analytical and Physical Chemistry Series. Lewis Publishers, 554 pp.

Burgess, B.A., Chasteen, N.D., Gaudette, H.E., 1975. Electron paramagnetic resonance spectroscopy: a suggested approach to trace metal analyses in marine environments. Environ. Geol. 25, 163–181.

Carpenter, R., 1983. Quantitative electron spin resonance (ESR) determinations of forms and total amounts of Mn in aqueous environmental samples. Geochim. Cosmochim. Acta 47, 875–885.

Cases, J.M., Liétard, O., Yvon, J., Delon, J.F., 1982. Etude des propriétés cristallochimiques, morphologiques, superficielles de kaolinites désordonnées. Bull. Mineral. 105, 439–455.

Cheshire, M.V., Senesi, N., 1998. Electron spin resonance spectroscopy of organic and mineral soil particles. Structure and Surface Reactions of Soil Particles. In: Huang, P.M., Senesi, N., Buffle, J. (Eds.), IUPAC Ser. 4 Wiley, Chichester, UK, pp. 325–374.

Clozel, B., Allard, T., Muller, J.P., 1994. Nature and stability of radiation-induced defects in natural kaolinites : new results and a reappraisal of published works. Clays Clay Miner. 42, 657–666.

Dai, M.H., Martin, J.M., 1995. First data on trace metal level and behaviour in two major Arctic river-estuarine systems (Ob and Yenisey) and in the adjacent Kara Sea, Russia. Earth Planet. Sci. Lett. 131, 127–141.

De Vitre, R., Davison, W., 1993. Manganese particles in freshwater. In: Buffle, J., Van Leuwen, H.P. (Eds.), Environ. Part. 2, Environ. Anal. Phys. Chem. Ser. Lewis Publishers, Boca Raton, USA, pp. 317–353.

Dupré, B., Gaillardet, J., Rousseau, D., Allègre, C.J., 1996. Major and trace elements of river-borne material: the Congo basin. Geochim. Cosmochim. Acta 60 (8), 1301–1321.

Eisma, D., 1993. Suspended Matter in the Aquatic Environment. Springer-Verlag, Berlin, 315 pp.

Eyrolle, F., Benedetti, M., Benaim, J.Y., Fevrier, D., 1996. The distribution of colloidal and dissolved organic carbon, major elements and trace elements in small tropical catchments. Geochim. Cosmochim. Acta 60, 3643–3656.

Farmer, V.C., Palmieri, P., 1975. The characterization of soil minerals by infrared spectroscopy. In: Gieseking, J.E. (Ed.), Soil Components. Inorganic Components Vol. 2, Springer-Verlag, New York, pp. 573–671.

Gaillardet, J., Dupré, B., Allègre, C.J., 1995. A geochemical mass budget model applied to the Congo basin rivers. Erosion rates and composition of the Continental crust. Geochim. Cosmochim. Acta 59 (17), 3469–3485.

Gerasimowicz, W.V., Byler, M.D., Susi, H., 1986. Resolution-enhanced FT-IR spectra of soil constituents : humic acid. Appl. Spectrosc. 40, 504–506.

Gibbs, R.J., 1973. Mechanisms of trace metal transport in rivers. Science 180, 71–73.

Giresse, P., Ouetiningue, R., Barusseau, J.P., 1990. Minéralogie et micro-granulométrie des suspensions et des alluvions du Congo et de l'Oubangui. Sci. Géol., Bull. 43 (2–4), 151–173, Strasbourg.

Goodman, B.A., Hall, P.L., 1994. Electron paramagnetic resonance spectroscopy. In: Wilson, M.J. (Ed.), Clay Mineralogy: Spectroscopic and Chemical Determination Methods. Chapman & Hall, London, 367 pp.

Graetsch, H., Gies, H., Topalovic, I., 1994. NMR, XRD and IR study on microcrystalline opals. Phys. Chem. Miner. 21, 166–175.

Hart, B.T., Douglas, G.B., Beckett, R., Van Put, A., Van Griecken, R.E., 1993. Characterization of colloidal and particulate matter transported by the Magela Creek system, Northern Australia. Hydrol. Processes 7, 105–118.

Hawthorne, F.C., 1988. Spectroscopic methods in Mineralogy and Geology, Mineralogical Society of America. Rev. Mineral. 18, 698 pp.

Iler, R.K., 1979. The Chemistry of Silica. Solubility, Polymerization, Colloid, and Surface Properties and Biochemistry. Wiley-Interscience, 761 pp.

Jenne, E.A., 1968. Controls on Mn, Fe, Co, Ni, Cu and Zn concentrations in soils and water: the significant role of hydrous Mn and Fe oxides. In: Baker, R.A. (Ed.), Trace Inorganics in Water. Am. Chem. Soc. 73 Washington, pp. 334–387.

Johnson, C.A., 1986. The regulation of trace element concentrations in river and estuarine waters contaminated with acid mine drainage: the adsorption of Cu and Zn on amorphous Fe oxyhydroxides. Geochim. Cosmochim. Acta 50, 2433–2438.

Kodama, H., Schnitzer, M., 1967. X-ray studies of fulvic acids, a soil humic compounds. Fuel. J. Fuel Sci. 46, 87–94.

Kostka, J.E., Luther III, G.W., Nealson, K.H., 1995. Chemical and biological reduction of Mn(III)-pyrophosphate complexes: potential importance of dissolved Mn(III) as an environmental oxidant. Geochim. Cosmochim. Acta 59, 885–894.

Laxen, D.P.H., Davison, W., Woof, C., 1984. Manganese chemistry in rivers and streams. Geochim. Cosmochim. Acta 48, 2107–2111.

Leenheer, J.A., Noyes, T.I., 1989. Derivatization of humic substances for structural studies. In: Hayes, M.H.B., MacCarthy, P., Malcolm, R.L., Swift, R.S. (Eds.), Humic Substances II. Wiley, 764 pp.

Lucas, Y., Nahon, D., Cornu, S., Eyrolle, F., 1996. Genèse et fonctionnement des sols en milieu équatorial. C.R. Acad. Sci. Paris 322, 1–16.

Malengreau, N., Muller, J.P., Calas, G., 1994. Fe-speciation in kaolins : a diffuse reflectance study. Clays Clay Miner. 42 (2), 137–147.

Malengreau, N., Muller, J.P., Calas, G., 1995. Spectroscopic approach for investigating the status and mobility of Ti in kaolinitic materials. Clays Clay Miner. 43 (5), 615–621.

McBride, M., 1982. Electron spin resonance investigation of Mn^{2+} complexation in natural and synthetic organics. Soil Sci. Soc. Am. J. 46, 1137–1142.

Muller, J.P., Calas, G., 1993a. Mn^{2+} bearing kaolinites from

lateritic weathering profiles: geochemical significance. Geochim. Cosmochim. Acta 57, 1029–1037.

Muller, J.P., Calas, G., 1993b. Genetic significance of paramagnetic centers in kaolinites. In: Murray, H.H., Bundy, W., Harvey, C. (Eds.), Kaolin Genesis and Utilization. Clay Minerals Society, Boulder, pp. 261–289.

Muller, J.P., Manceau, A., Calas, G., Allard, T., Ildefonse, P., Hazemann, J.L., 1995. Crystal chemistry of kaolinite and Fe–Mn oxides: relation with formation conditions of low temperature systems. Am. J. Sci. 295, 1115–1155.

Nkounkou, R.R., Probst, J.L., 1987. Hydrology and geochemistry of the Congo river system. Mitt. Geol. Palaeontol. Inst. Univ. Hamburg 64, 483–508, SCOPE/UNEP Sonder bd.

Olivié-Lauquet, G., 1996. Analyse des transferts solides dans la géosphère tropicale: exemple du bassin versant du Nyong (Cameroun). Thesis, Paris 7 Univ., France.

Olivié-Lauquet, G., Allard, T., Benedetti, M., Muller, J.P., 1999. Chemical distribution of trivalent iron in riverine material from a tropical ecosystem: a quantitative EPR study. Water Res. 33, 2726–2734.

Perret, D., Newman, M.E., Nègre, J-C., Chen, Y., Buffle, J., 1994. Submicron particles in the Rhine river: I. Physico-chemical characterisation. Water Res. 28 (1), 91–106.

Piccolo, A., Stevenson, F.J., 1982. Infrared spectra of Cu^{2+}, Pb^{2+}, and Ca^{2+} complexes of soil humic substances. Geoderma 27, 195–208.

Piperno, D.R., 1987. Phytoliths Analysis. An Archeological and Geological Perspective. Academic Press, 275 pp.

Salomons, W., Forstner, U., 1984. Metals in the Hydrosphere. Springer-Verlag, Heildelberg.

Sarazin, G., Ildefonse, Ph., Muller, J.P., 1982. Contrôle de la solubilité du fer et de l'aluminium en milieu ferralitique. Geochim. Cosmochim. Acta 52, 1267–1279.

Scheinost, A.C., Chavernas, A., Barron, V., Torrent, J., 1998. Use and limitations of second-derivative diffuse reflectance spectroscopy in the visible to near-infrared range to identify and quantify Fe oxide minerals in soils. Clays Clay Miner. 46, 528–536.

Senesi, N., 1992. Metal-humic substance complexes in the environment. Molecular and mechanistic aspects by multiple spectroscopic approach. In: Adriano, D.C. (Ed.), Biogeochemistry of Trace Metals. Lewis Publishers, pp. 429–497.

Sholkovitz, E.R., 1992. Chemical evolution of rare earth elements: fractionation between colloidal and solution phases of filtered river water. Earth Planet Sci. Lett. 114, 77–84.

Stallard, R.F., 1988. Weathering and erosion in the humid tropics. In: Meybeck, L. (Ed.), Physical and Chemical Weathering in Geochemical Cycles. Kluwer Academic Press.

Stevenson, F.J., Goh, K.M., 1971. Infra-red spectra of humic acids and related substances. Geochim. Cosmochim. Acta 35, 471–483.

Tessier, A., Fortin, D., Belzile, N., DeVitre, D.D., Leppard, G.G., 1996. Metal sorption to diagenetic iron and manganese oxyhydroxides and associated organic matter: narrowing the gap between field and laboratory measurements. Geochim. Cosmochim. Acta 60, 387–404.

Viers, J., Dupré, B., Polvé, M., Schott, J., Dandurand, J-L., Braun, J-J., 1997. Chemical weathering in the drainage basin of a tropical watershed (Nsimi–Zoetele site, Cameroun): comparison between organic-poor and organic-rich waters. Chem. Geol. 140, 181–206.

Vinkler, P., Lakatos, B., Meisel, J., 1976. Infrared spectroscopic investigations of humic substances and their metal complexes. Geoderma 15, 231–242.

Wendlandt, W.W.M., Hecht, H.G., 1966. Reflectance Spectroscopy. Interscience Publishers, Wiley, New York, 298 pp.